A MULTIPHASE FLOW APPROACH AND A SINGLE-PHASE FLOW APPROACH IN THE CONTEXT OF A EULER MODEL FOR PRIMARY BREAK-UP

P.-A. Beau°*, R. Lebas*, M. Funk°, F.-X. Demoulin*

CORIA-University of Rouen, 76801 Saint-Etienne du Rouvray Cedex, France
E-mail beau@coria.fr, tel 33 (0)2 32 95 37 24, fax 33 (0)2 32 95 37 98

° Sce 64240 – Technocentre RENAULT, Batiment le Gradient,1 avenue du golf, 78288 Guyancourt cedex, France
tel 33 (0)1 34 95 24 60, fax 33 (0)1 34 95 77 16

ABSTRACT

Atomizing systems must be able to form sprays with predetermined characteristics. These are affected by the shape of the injector as well as by external conditions. Thus, in order to avoid numerous experiments, it is necessary to develop predictive atomization models able to deal with the complete atomization process. This can be done using a Eulerian primary break-up model. This approach describes the flow continuously from inside the injector to the dispersed spray region. In this paper the Eulerian multiphase approach and the Eulerian single-phase approach are compared and the results lead to an intermediate quasi-multiphase approach.

Introduction

The primary break-up in spray applications is a complex phenomenon. It involves very strong coupling between the liquid and the gas phases. A predictive model for the atomization process is presented in this article. This model, based on a single-phase Euler model, describes the whole process from inside the injector to the final dilute spray region. Initially, the classical transport equations of the mean mixture variable are proposed. Unclosed correlation terms appear in the set of equations. The k-ε model is used to model the turbulence. The work particularly emphasizes the treatment of the turbulent flux, generally treated as diffusion. Different closure laws are defined: gradient closure, single-phase closure and drag law closure. The limitations of the classical gradient law closure are shown. To overcome these limitations, the exact transport equation of the diffusion flux is considered. The unclosed terms involved in this equation can be modelled either from the single-phase point of view or by adapting the multiphase approach. This last method is used in the so-called quasi-multiphase closure by introducing a drag law term. Finally, the three different approaches are implemented and the numerical results are compared with the experimental results.

1. Equations of the model

This approach considers the liquid phase and the gas phase as a single mixture. Average field equations for the mixture phase are obtained by averaging the local conservation equation. Thus the continuity equation is classically written:

$$\frac{\partial \overline{\rho}}{\partial t} + \frac{\partial \overline{\rho}\widetilde{U}_j}{\partial x_j} = 0 \ . \tag{1}$$

$\overline{\rho}$ represents the mean mixture density, $\widetilde{U}_j = \widetilde{X}_2 U_{2,j} + \widetilde{X}_1 U_{1,j}$ is the Favre averaged mixture velocity and $\widetilde{X}_2$ and $\widetilde{X}_1$ stand respectively for the Favre average of the liquid and the gas mass fractions. Mean gas and liquid velocities (respectively $U_{1,j}$ and $U_{2,j}$) are defined by considering the multiphase approach [1].

The density of the gas and liquid are both considered to be constant. The state equation for the density is

$$\frac{1}{\overline{\rho}} = \frac{\widetilde{X}_2}{\rho_2} + \frac{\widetilde{X}_1}{\rho_1} \ . \tag{2}$$

The equation for the mean mixture velocity $\widetilde{U}_i$ obeys a classical conservation equation, which does not involve any terms corresponding to gas-liquid exchanges at the interface [2] because the mean velocity of the liquid and gas phases is not taken into account.

$$\frac{\partial \overline{\rho}\widetilde{U}_i}{\partial t} + \frac{\partial \overline{\rho}\widetilde{U}_j\widetilde{U}_i}{\partial x_j} = -\frac{\partial \overline{P}}{\partial x_i} - \frac{\partial \overline{\rho u_i'' u_j''}}{\partial x_j}$$

(3)

In this equation, u_i'' represents the fluctuation of the mixture velocity. $\overline{P}$ is the mean pressure. This equation contains a stress term that has to be modelled. The viscous forces in the mixture phase have been neglected with respect to the stress term because the Reynolds number is large.

In order to calculate the dispersion of the liquid phase, the equation for the liquid mass fraction $\widetilde{X}_2$ is defined. The balance equation for the mean liquid mass fraction $\widetilde{X}_2$ is obtained in the same way as for a passive scalar in a gas but neglecting molecular diffusion.

$$\frac{\partial \overline{\rho}\widetilde{X}_2}{\partial t} + \frac{\partial \overline{\rho}\widetilde{U}_j\widetilde{X}_2}{\partial x_j} = -\frac{\partial \overline{\rho u_j'' x_2''}}{\partial x_j}$$

(4)

x_2'' is the fluctuation of the liquid mass fraction. The term on the RHS of Eq.(4) represents the diffusion flux of the liquid. This diffusion flux is directly linked with the gas an the liquid velocities by considering the exact equation

$$\overline{\rho u_i'' x_2''} = \overline{\rho}\widetilde{X}_2\widetilde{X}_1(U_{2,i} - U_{1,i}) .$$

(5)

By envisaging the transport equation for the turbulent diffusion flux, the multiphase approach becomes equivalent to the single-phase approach. This is shown in Table 1.

Multiphase approach	Quasi multiphase approach
Liquid momentum equation U_2	Equation for $\widetilde{U} = \widetilde{X}_2 U_2 + \widetilde{X}_1 U_1$
Gas momentum equation U_1	Equation for $\overline{\rho u'' x_2''} = \overline{\rho}\widetilde{X}_2\widetilde{X}_1(U_2 - U_1)$
Liquid mass equation $\rho_2\overline{X}_2$	Equation for $1/\overline{\rho} = \widetilde{X}_2/\rho_2 + \widetilde{X}_1/\rho_1$
Gas mass equation $\rho_1\overline{X}_1$	Equation for $\overline{\rho}\widetilde{X}_2$

Table 1: The equivalence between the multiphase and the quasi-multiphase approaches

2. Modelling of the unclosed terms

The dynamics of the spray is controlled by the four previous equations. Equations (1) and (2) are closed, but in equations (3) and (4) unclosed correlation terms appear. The closure model used is significant for the description of the spray especially for the turbulent diffusion flux of the liquid mass fraction because it deals with the drift between the two phases.

2.1. Modelling of the Reynolds stress tensor $\overline{\rho u_i'' u_j''}$

The classical single-phase k-ε turbulence model [3] for such a flow is used. Here the definition of $\widetilde{k}$ and $\widetilde{\varepsilon}$ do not distinguish the liquid from the gas phase. Only the global turbulence of the gas-liquid mixture is considered. The Boussinesq eddy viscosity concept is used, leading to the following model for the Reynolds stress tensor:

$$\overline{u_i'' u_j''} = -v_t(\frac{\partial \widetilde{U}_i}{\partial x_j} + \frac{\partial \widetilde{U}_j}{\partial x_i} - \frac{2}{3}\frac{\partial \widetilde{U}_k}{\partial x_k}\delta_{ij}) + \frac{2}{3}\widetilde{k}\delta_{ij} ,$$

(6)

where $v_t = C_\mu\frac{\widetilde{k}^2}{\widetilde{\varepsilon}}$ is the turbulent viscosity and δ_{ij} the Kronecker symbol.

2.2. Modelling of the turbulent diffusion flux $\overline{\rho u_j'' x_2''}$

By analogy with Fick's law, the proportionality to the mean gradient could be employed for the diffusion flux:

$$\overline{\rho u_i'' x_2''} = -\overline{\rho}\,\frac{\nu_t}{Sc_x}\,\frac{\partial \widetilde{X}_2}{\partial x_i} \tag{7}$$

with Sc_x a turbulent Schmidt number and ν_t the turbulent viscosity. This model is called Model 1 in the following.

A more elaborate approach considers the transport equation for $\overline{\rho u_i'' x_2''}$. The gradient closure does not appear to be efficient for modelling the cases where the liquid and the gas phases are not in dynamic equilibrium (drift between the two phases). For instance, the diffusion law is not adapted to representing the slipping motion of a homogeneous liquid fraction field (droplet cloud). The liquid mass fraction gradient is nil although the diffusion flux is not nil because there is a drift velocity between the gas and the liquid (See Eq.(5)). Thus the gradient law is not sufficient.

By considering instantaneous mass and momentum balance equations, the exact transport equation for the turbulent diffusion flux is obtained.

$$
\begin{aligned}
\frac{\partial \overline{\rho u_i'' x_2''}}{\partial t} + \frac{\partial \widetilde{U}_j \overline{\rho u_i'' x_2''}}{\partial x_j} = & -\frac{\partial \overline{\rho u_j'' u_i'' x_2''}}{\partial x_j} - \frac{\partial \overline{p' x_2''}}{\partial x_i} + \frac{\partial \overline{\rho \sigma_{ij}'' x_2''}}{\partial x_j} - \overline{\rho u_i'' u_j''}\,\frac{\partial \widetilde{X}_2}{\partial x_j} \\
& - \overline{\rho u_j'' x_2''}\,\frac{\partial \widetilde{U}_i}{\partial x_j} - \overline{x_2''}\,\frac{\partial \overline{P}}{\partial x_i} - \overline{\rho \sigma_{ij}\,\frac{\partial X_2}{\partial x_j}} + \overline{\rho}\widetilde{\sigma}_{ij}\,\frac{\partial \widetilde{X}_2}{\partial x_j} + \overline{P\,\frac{\partial X_2}{\partial x_i}} - \overline{P}\,\frac{\partial \overline{X}_2}{\partial x_i}
\end{aligned}
\tag{8}
$$

$\widetilde{\sigma}_{ij}$ and σ_{ij}'' are respectively the stress tensor and the stress tensor fluctuations.

The first three terms of the RHS of the transport equation correspond to the turbulent diffusion. A gradient law closure is employed.

$$-\overline{\rho u_j'' u_i'' x_2''} - \overline{p' x_2''}\delta_{ij} + \overline{\rho \sigma_{ij}'' x_2''} = \frac{\nu_t}{Sc_2}\,\frac{\partial \overline{\rho u_i'' x_2''}}{\partial x_j} \tag{9}$$

Sc_2 is a turbulent Schmidt number.

The calculation of $\overline{x_2''}$ results exactly in

$$\overline{x_2''} = \overline{\rho}\widetilde{X}_2 \widetilde{X}_1 \left(\frac{1}{\rho_2} - \frac{1}{\rho_1}\right). \tag{10}$$

The last four terms of the RHS of the equation (called IT for Interfacial Transfer) correspond to the momentum transfer between the gas and the liquid phases i.e. they express the contributions of stress tensor fluctuations and pressure fluctuations on the liquid-gas interface. This equation can be modelled considering the multiphase or the single-phase models.

2.2.1. The single-phase closure

According to the previous work [2], the interfacial terms for the single-phase approach are closed following the work of Bailly et al.. The correction added to that closure by Blokkeel et al. [4] is also incorporated.

$$IT = +\gamma_x \overline{\rho u_j'' x_2''}\,\frac{\partial \widetilde{U}_i}{\partial x_j} - \gamma_x' \overline{x_2''}\,\frac{\partial \overline{P}}{\partial x_i} - \frac{\overline{\rho}}{\tau_t}\underbrace{\left(a_1 \frac{\overline{\rho u_i'' x_2''}}{\overline{\rho}} + \frac{C_y}{C_\mu}\,\frac{\overline{x_2''}}{\widetilde{X}_2 \widetilde{X}_1}\,\nu_t\,\frac{\partial \widetilde{X}_2}{\partial x_i}\right)}_{Main\ terms} \tag{11}$$

$\tau_t = \widetilde{k}/\widetilde{\varepsilon}$ is the characteristic turbulent time. γ_x, γ_x', C_y and a_1 are constants usually taken as 0.5, 0.5, 0.33 and 5. This model is called Model 2.

2.2.2. The multiphase closure

By following the multiphase approach, where the liquid phase is generally considered as a set of droplets, the interfacial transfer term can be expressed in terms of a drag law closure. A new characteristic time scale is considered: the drag time scale $\tau_D = \rho_2 / \rho_1 F_D$. The interfacial transfer expression becomes:

$$IT = -\frac{\rho_2 \widetilde{X}_2}{\tau_D}(U_{2,i} - U_{1,i} + D_t \frac{\partial \widetilde{X}_2}{\partial x_i}) = -\frac{\overline{\rho}}{\widetilde{X}_1 \tau_D}(\frac{\overline{\rho u_i'' x_2''}}{\overline{\rho}} + D_t \frac{\partial \widetilde{X}_2}{\partial x_i}) . \tag{12}$$

D_t is a turbulent diffusion coefficient. The expression of this turbulent coefficient differs according to each author's approach. Iyer et al. [5] use the turbulent diffusivity of the liquid (multiphase model). Simonin [6] uses the fluid-particle turbulent dispersion tensor. The expression retained for the turbulent diffusion coefficient is $D_t = \nu_t / Sc_3$, with Sc_3 being a turbulent Schmidt number. The multiphase closure is quite similar to the single-phase closure. The turbulent time scale in Eq.(11) is replaced by a drag time scale in Eq.(12). The drag term closure, however, may not be sufficient in the region near the injector nozzle because the drag laws considered were developed for droplets (dispersed spray region) and not for liquid filaments (dense spray region). F_D is the average drag coefficient. The expression retained by Simonin is used in the present work. A characteristic length is necessary in the expression of the average drag coefficient. Thus, a new equation is added to the global model: the transport equation for the liquid surface density $\overline{\Sigma}$. The characteristic length, used in the drag law, is the Sauter mean diameter, which is obtained with the following expression: $\overline{d}_{32} = 6\overline{\rho}\widetilde{X}_2 / (\rho_2 \overline{\Sigma})$. As for the flame surface density, the equation for $\overline{\Sigma}$ is postulated [2]. This drag law closure is used in the case of atomization. Near the nozzle, the liquid fraction is close to one and it is perhaps more realistic to use a drag law for bubbles in liquid rather than a drag law for liquid droplets in gas. This quasi-multiphase model is called Model 3 in the following.

3. Comparisons with experiments

3.1. Experimental conditions

In this part, comparisons of computed and measured results from the experimental data of Wu et al. [7] are presented. These data consist in measurements of axial drop velocity in steady sprays. The liquid (n-hexane) is injected into quiescent nitrogen at room temperature but at high pressure such that the ratio of the gas density to the injected fuel density is similar to that in a Diesel engine cylinder at the top dead center. The experimental conditions are presented in Table 2. The experimental apparatus is detailed in the paper of Wu et al.. The diameter of the injector is $D=127$ μm.

Case	P (Mpa)	ρ_1 (kg m^{-3})	U_{inj} (m s^{-1})
A	4.24	48.68	127
B	1.48	17.024	127

Table 2: Experimental conditions used in the experiments of Wu et al.

The measurements of the mean and fluctuating axial velocities were reported at axial locations along the chamber axis at x/D=400,600.

3.2. Computational conditions

The comparison with the experimental data is performed in an axisymetric half chamber. The computations were performed using the CFD code Star-CD VERSION 3.15. The computational grid is shown in figure 1. The axial and radial grid resolution is non-uniform. The total number of cells is 100*50. There are 10 cells along the diameter of the injector hole. The aspect ratio of the cells near the orifice is close to one in order to achieve good numerical accuracy.
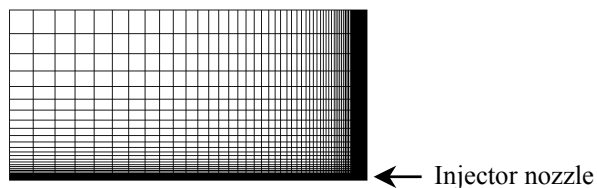

←— Injector nozzle

Figure 1: The computational grid

3.3. Results and discussions

The three models computed in this work are quite efficient for the description of the dynamics of the spray when compared to the experimental data available. Nevertheless different behaviours are observed. The measurements of Wu et al. are far from the injector nozzle to avoid the region where the spray is optically dense. At this location, the effect of the model are smoothed because the dynamic equilibrium between the gas phase and the liquid phase is almost reached. Figure 2 illustrates this phenomenon. As there is no drift between the two phases, the gradient law closure is sufficient.

Nevertheless, differences appear between the models on figure 3. In case A, the dynamic equilibrium is reached farther from the injector. For x/D=400, a better efficiency of the drag law closure model is shown. Model 3 is the only one able to represent the slip velocity between the liquid and the gas phases. Further from the axis, however, the most efficient model is Model 2. These two observations reveal the dynamics of the spray. In the dense spray region, the diffusion flux of the liquid fraction is controlled by the drag acting on the liquid droplets. In the dilute spray region, i.e. further from the injector axis, the diffusion flux is controlled by the turbulence phenomenon.
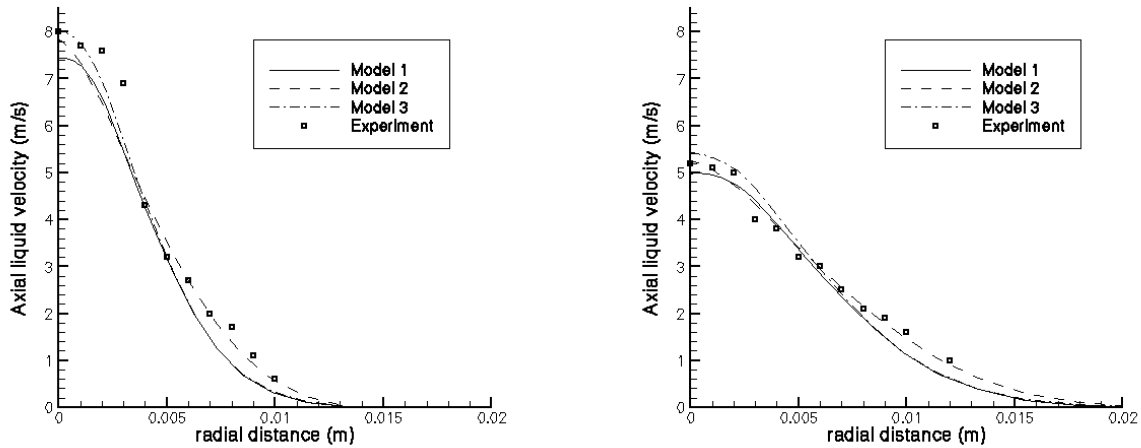

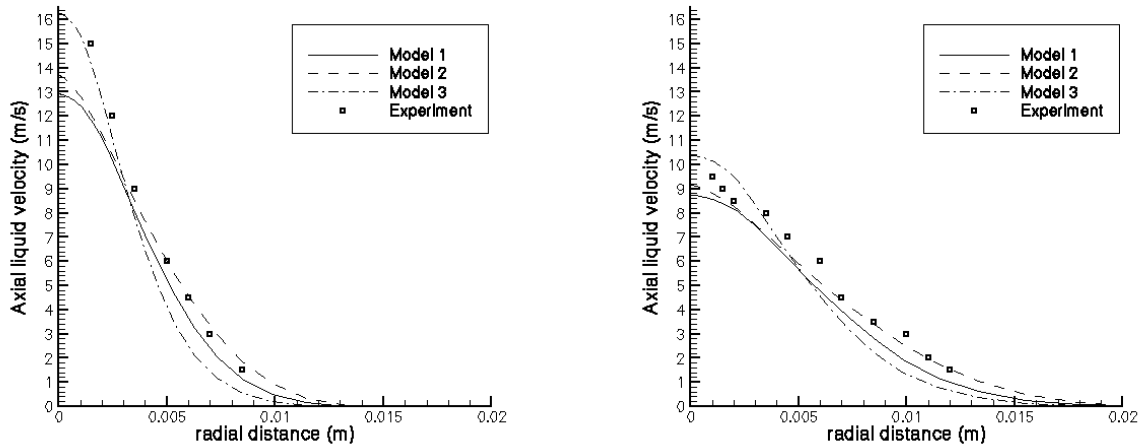*Figure 2: Axial liquid velocity versus radial distance at x/D=400 and x/D=600 for case A*

Figure 3: Axial liquid velocity versus radial distance at x/D=400 and x/D=600 for case B

The importance of the time scale in the spray is illustrated by Figure 4. This figure represents the drag time scale and the turbulent time scale versus the radial distance of the injector axis. The time scale governing the physical phenomena is the higher time scale. Thus, the influence of the drag phenomenon is more important in the injector axis region, i.e. the fully dense spray region where the slip velocity is not nil. In the dispersed region, the turbulent time scale is higher, thus the governing phenomenon is the turbulence.

Figure 5 compares the behaviour of the three models in the dense spray region, near the injector hole at x/D=100. There is no equilibrium between the gas and liquid phases. Thus, the results given by the models are very different, showing that, in order to obtain the actual liquid dispersion, it is important to represent the turbulent diffusion of the liquid correctly.
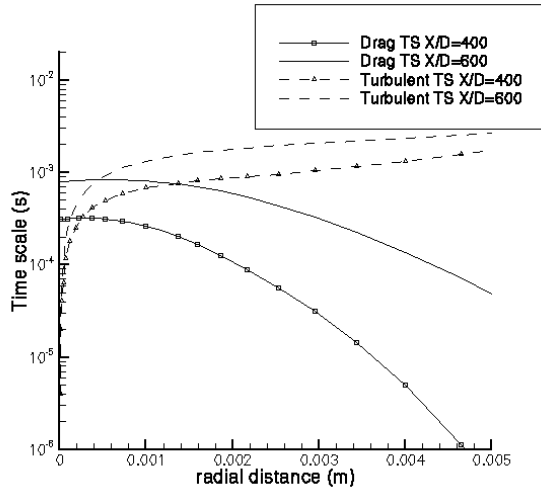
Figure 4: Drag and turbulent time scales versus
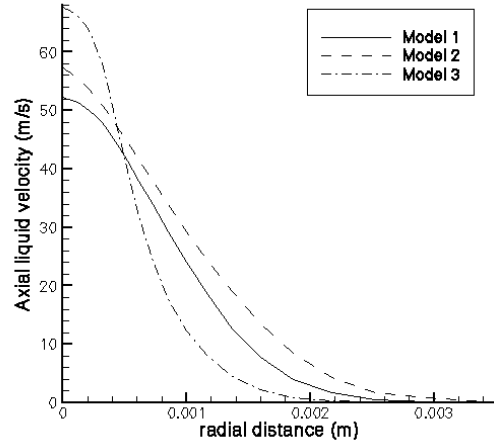radial distance at x/D=400 and x/D=600 for case B

Figure 5: Axial liquid velocity versus
radial distance at x/D=100 for case B

Conclusion

A Eulerian model for the atomization process of a liquid jet has been proposed in this paper. The transport equation for the liquid fraction was developed with particular emphasis on the diffusion flux. Three closure models were introduced. The limitations of the classical gradient law closure were explained. The new closure based on multiphase flow development was applied. It was difficult to validate the model because of the lack of precise experimental data near the injector nozzle. Nevertheless, a better behaviour of the drag law model is obtained, where the slip velocity is high and the second order model based on the turbulent time scale is better, where the dynamic equilibrium is reached.

Acknowledgments

NOMENCLATURE

D	diameter of the injector [m]	$U_{2,j}$	mean liquid velocity [m s^{-1}]	ρ_2	liquid density [kg m^{-3}]
D_t	turbulent diffusion coefficient [m^2 s^{-1}]	u_i''	fluctuating mixture velocity [m s^{-1}]	$\widetilde{\sigma}_{ij}$	stress tensor [s^{-1}]
$\overline{d}_{32}$	Sauter mean diameter [m]	$\widetilde{X}_1$	averaged gas mass fraction [-]	σ_{ij}''	fluctuating stress tensor [s^{-1}]
$\overline{P}$	mean pressure [Pa]	$\widetilde{X}_2$	averaged liquid mass fraction [-]	$\overline{\Sigma}$	surface density [m^{-1}]
Sc	Schmidt number [-]	δ_{ij}	Kronecker symbol [-]	τ_t	characteristic turbulent time [s]
$\widetilde{U}_j$	Favre averaged mixture velocity [m s^{-1}]	$\overline{\rho}$	mean mixture density [kg m^{-3}]	τ_D	drag time scale [s]
$U_{1,j}$	mean gas velocity [m s^{-1}]	ρ_1	gas density [kg m^{-3}]	ν_t	turbulent viscosity [m^2 s^{-1}]

REFERENCES

1. Drew D.A., Mathematical modelling of two-phase flow, Annual review of fluid mechanics, vol. 15, pp. 261-291.
2. Vallet A., Burluka A.A., Borghi R., Development of a Eulerian model for the atomization of a liquid jet, Atomization and Sprays, vol. 11, pp. 619-642,2001.
3. Launder B.E., Spalding D.B., The numerical computation of turbulent flows, Comp. Methods in applied mechanics and engineering, vol. 3, pp. 345-353, 1974.
4. Blokkeel G. et al., A continuous modelling approach for describing the atomization process from inside the injector to the final spray, ICLASS, 2003.
5. Iyer V., Abraham J., an evaluation of a two-fluid Eulerian-liquid Eulerian-gas model for Diesel sprays, Journal of fluids engineering, vol. 125, pp. 660-669,2003.
6. Simonin O., Continuum modelling of dispersed turbulent two phase flows, Combustion and turbulence in two phase flows, VKI lecture series, 1996-02.
7. Wu K.-J. et al., LDV measurements of drop velocity in Diesel-type sprays, AIAA Journal, vol. 22, no. 9, pp. 1263-1270,1984.